

Carbon and Chlorine Isotope Analysis to Identify Abiotic Degradation Pathways of 1,1,1-Trichloroethane

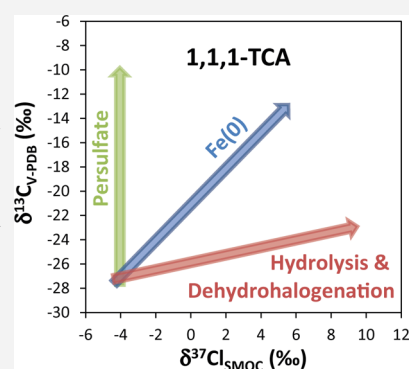
Jordi Palau,^{*,†} Orfan Shouakar-Stash,^{‡,§} and Daniel Hunkeler[†]

[†]Centre for Hydrogeology and Geothermics, University of Neuchâtel, Neuchâtel CH-2000, Switzerland

[‡]Department of Earth and Environmental Sciences, University of Waterloo, Waterloo N2L 3G1, Canada

[§]Isotope Tracer Technologies Inc., Waterloo, Ontario, Canada N2V 1Z5

ABSTRACT: This study investigates dual C–Cl isotope fractionation during 1,1,1-TCA transformation by heat-activated persulfate (PS), hydrolysis/dehydrohalogenation (HY/DH) and Fe(0). Compound-specific chlorine isotope analysis of 1,1,1-TCA was performed for the first time, and transformation-associated isotope fractionation $\epsilon_{\text{bulk}}^{\text{C}}$ and $\epsilon_{\text{bulk}}^{\text{Cl}}$ values were $-4.0 \pm 0.2\text{‰}$ and no chlorine isotope fractionation with PS, $-1.6 \pm 0.2\text{‰}$ and $-4.7 \pm 0.1\text{‰}$ for HY/DH, $-7.8 \pm 0.4\text{‰}$ and $-5.2 \pm 0.2\text{‰}$ with Fe(0). Distinctly different dual isotope slopes ($\Delta\delta^{13}\text{C}/\Delta\delta^{37}\text{Cl}$): ∞ with PS, 0.33 ± 0.04 for HY/DH and 1.5 ± 0.1 with Fe(0) highlight the potential of this approach to identify abiotic degradation pathways of 1,1,1-TCA in the field. The trend observed with PS agreed with a C–H bond oxidation mechanism in the first reaction step. For HY/DH and Fe(0) pathways, different slopes were obtained although both pathways involve cleavage of a C–Cl bond in their initial reaction step. In contrast to the expected larger primary carbon isotope effects relative to chlorine for C–Cl bond cleavage, $\epsilon_{\text{bulk}}^{\text{C}} < \epsilon_{\text{bulk}}^{\text{Cl}}$ was observed for HY/DH and in a similar range for reduction by Fe(0), suggesting the contribution of secondary chlorine isotope effects. Therefore, different magnitude of secondary chlorine isotope effects could at least be partly responsible for the distinct slopes between HY/DH and Fe(0) pathways. Following this dual isotope approach, abiotic transformation processes can unambiguously be identified and quantified.



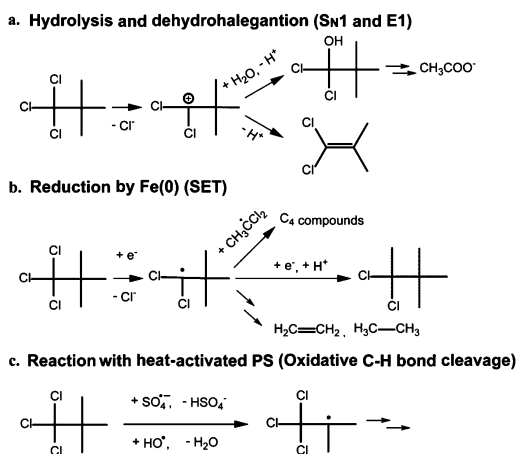
INTRODUCTION

Chlorinated ethanes are common groundwater contaminants, and 1,1,1-trichloroethane (1,1,1-TCA) has been found in at least half of the 1,662 National Priorities List sites identified by the U.S. Environmental Protection Agency (USEPA).^{1,2} 1,1,1-TCA has been widely used as a solvent, and its presence in the subsurface mainly results from industrial activity. In groundwater, 1,1,1-TCA may be transformed via multiple biotic and abiotic reaction pathways,^{3,4} making it challenging to identify degradation processes. Identifying processes is further complicated by the possibility of having the same products from different precursors. Abiotic 1,1,1-TCA degradation may yield daughter products such as 1,1-dichloroethene (1,1-DCE), ethene or ethane that can be formed from different precursors in sites impacted by a mixture of chlorinated compounds.^{4,5} In this case, parent–daughter relationships based solely on concentration data may lead to erroneous interpretations. Therefore, development of innovative methods for the elucidation of 1,1,1-TCA abiotic degradation pathways in the environment as well as in engineered systems is warranted.

Reported sequential anaerobic biodegradation of 1,1,1-TCA generally stalls at the stage of chloroethane (CA),^{6–8} a persistent groundwater contaminant considered as priority pollutant by the USEPA.⁹ Therefore, abiotic reactions of 1,1,1-TCA yielding nonchlorinated products are of special interest. In groundwater, 1,1,1-TCA is abiotically dechlorinated to acetate

(Ac) and 1,1-DCE by hydrolysis (nucleophilic substitution) and dehydrohalogenation (β -elimination), respectively.^{10,11} Hydrolysis and dehydrohalogenation (HY/DH) may proceed either via two parallel reactions starting from the substrate ($S_{\text{N}}2$ vs E2) or via a common pathway through formation of a carbocation intermediate (Scheme 1a).¹² However, according to the results from previous reaction studies,^{11–13} the second mechanistic scenario seems more likely. In anoxic conditions, 1,1,1-TCA can also undergo metal-catalyzed reduction by natural reductants such as iron sulfides.^{14,15} Transformation of 1,1,1-TCA by zero-valent metals and bimetallic reductants has been investigated to evaluate their potential application to in situ treatment techniques such as nanoparticles injection or permeable reactive barriers.^{16–20} For 1,1,1-TCA reductive dechlorination by zero-valent iron, cleavage of a C–Cl bond by dissociative single electron transfer (SET) and formation of 1,1-dichloroethyl radical intermediate has been proposed as the first reaction step (Scheme 1b), leading to the production of 1,1-dichloroethane (1,1-DCA, via hydrogenolysis), ethene/ethane (α -elimination) and C_4 compounds (coupling).^{16,18} Furthermore, recently, 1,1,1-TCA degradation by activated

Scheme 1. Proposed Abiotic Degradation Pathways for 1,1,1-TCA^a



^aDots in structural formulas represent unpaired electrons.

persulfate (PS) using different methods such as base²¹ and heat^{22–25} activation was demonstrated. Thermal decomposition of PS generates reactive oxygen species²⁵ and, for reaction with 1,1,1-TCA, transformation via H abstraction²⁵ has been postulated (Scheme 1c). Previous studies^{23,24,26} suggested that thermally activated PS could be used for in situ chemical treatment of volatile organic compounds; however, a current limitation is the scarce knowledge of PS reaction pathways in the subsurface.²⁷

Due to the susceptibility of 1,1,1-TCA to abiotic transformations, two of the three pathways investigated in this study (Scheme 1) may occur simultaneously in the aquifer. In anoxic conditions, reduction of 1,1,1-TCA by natural reductants¹⁵ or engineered Fe(0) systems²⁸ can occur in addition to HY/DH. On the other hand, the rate of HY/DH will increase significantly during treatment of 1,1,1-TCA by heat-activated PS due to the raise of water temperature.¹⁰ In fact, thermal enhancement of HY/DH has recently been proposed for in situ remediation of 1,1,1-TCA.²⁹

Compound-specific isotope analysis (CSIA) is an innovative tool to investigate reaction mechanisms of organic contaminants and their degradation pathways in the environment because the extent of isotope fractionation (ϵ_{bulk}) during compound transformation is highly reaction-specific.^{30–34} For organic contaminants, transformation-induced isotope fractionation is generally larger than the one related to phase transfer processes such as sorption or volatilization.³⁵ Although isotope fractionation of one element alone (e.g., $\epsilon_{\text{bulk}}^{\text{C}}$) could provide pathway distinction in laboratory experiments,³⁶ it is not possible under field conditions. Here, contaminant concentration changes related to processes other than its transformation (such as sorption or dilution) cannot be excluded, preventing accurate calculation of ϵ_{bulk} values. Therefore, a dual isotope approach is necessary to differentiate contaminant degradation pathways in the field.³⁷ Recent development of analytical methods for online Cl-CSIA, either by continuous flow gas chromatography isotope ratio mass spectrometry (GC–IRMS)³⁸ or GC–quadrupole mass spectrometry (GC–qMS),^{37,39–41} has simplified the measurement of chlorine isotope ratios in chlorinated compounds.^{42,43} These new methods open new possibilities for a dual C–Cl isotope approach, which has not been applied to 1,1,1-TCA yet.

During the course of a reaction, combined changes in isotope ratios (e.g., $\Delta\delta^{13}\text{C}$ vs $\Delta\delta^{37}\text{Cl}$) for a given reactant generally yields a linear trend in a dual element isotope plot.^{44,45} The dual element isotope slope ($\Lambda = \Delta\delta^{13}\text{C}/\Delta\delta^{37}\text{Cl}$) reflects isotope effects of both elements³⁰ and, thus, different slopes may be expected for distinct transformation mechanisms involving different bonds with distinct elements. Following this approach, dual isotope slopes observed in the field can be compared to the slopes determined in laboratory experiments to identify degradation pathways. For a given compound, knowledge whether different abiotic reactions lead to characteristic slopes in dual C–Cl isotope plots is still very limited for chlorinated ethenes^{46–48} and, to our knowledge, currently nonexistent for chlorinated ethanes. This knowledge is a prerequisite for the application of a dual isotope approach to in situ contaminant studies.

In addition to the dual isotope approach, evaluation of underlying kinetic isotope effects (i.e., $\text{KIE} = k^{\text{L}}/k^{\text{H}}$, where k^{L} and k^{H} are the reaction rates of molecules containing the light and heavy isotopes, respectively) also yields insight into the reaction mechanisms. KIEs derived from ϵ_{bulk} values, so-called “apparent” kinetic isotope effects (AKIEs),⁴⁹ may then be compared to theoretical or typical intrinsic KIEs for a given reaction. However, reaction mechanisms sometimes cannot be clearly identified because experimental AKIEs may be smaller than the intrinsic KIE if the latter is masked due to nonfractionating rate limiting steps (such as mass transfer through the cell membrane or transport to the mineral reactive surfaces).³⁰ Therefore, increasing attention is paid to the dual isotope approach for improved differentiation of reaction mechanisms.^{44,45} A significant advantage of this approach is that Λ often remains constant, regardless of masking effects.^{50,51} The reason is that rate limiting preceding steps are generally nonfractionating so that both elements are masked to the same extent.⁴⁹ In this case, by taking the ratio of the isotope shift for the two elements (e.g., $\Delta\delta^{13}\text{C}/\Delta\delta^{37}\text{Cl}$) masking effects cancel out.

The main aims of this study were (i) to assess the potential of the dual C–Cl isotope approach for identifying abiotic degradation pathways of 1,1,1-TCA and (ii) to explore the underlying reaction mechanisms based on resultant dual isotope slopes and estimated ^{13}C and ^{37}Cl -AKIEs. We investigated dual element isotope fractionation of 1,1,1-TCA during HY/DH, reduction by microized Fe(0) and reaction with heat-activated PS in laboratory batch experiments. For the first time, isotope fractionation $\epsilon_{\text{bulk}}^{\text{Cl}}$ values (for all reactions) and $\epsilon_{\text{bulk}}^{\text{C}}$ (for HY/DH and reaction with heat-activated PS) were determined. In addition to isotope fractionation in the substrate, carbon isotope ratios of 1,1,1-TCA reaction products were also evaluated.

■ MATERIALS AND METHODS

Experimental Setup. All batch experiments were conducted in duplicate and reaction vials and controls were prepared at an initial 1,1,1-TCA concentration of 0.25 mM using a pure 1,1,1-TCA carbon isotopic working standard ($\delta^{13}\text{C}_0 = -26.3 \pm 0.1\%$, \pm standard deviation (1σ), number of measurements (n) = 5). A list of chemicals and additional experiment details is available in the Supporting Information.

Batch Experiments with PS. Reaction of 1,1,1-TCA with heat-activated PS (PS/1,1,1-TCA molar ratio of 90/1) was performed under controlled temperature (50 °C) using a thermostatic water bath. Reaction vials containing 42 mL of

aqueous solution and a minimal headspace (1 mL) were stirred at 200 rpm throughout the experiment. Control vials without PS were carried out in parallel.

HY/DH Batch Experiments. Reaction of 1,1,1-TCA in water was conducted at 50 °C in order to increase its reaction rate relative to the rate at ambient temperature (i.e., half-lives ($t_{1/2}$) from 1.1 years at 25 °C to 3.6 days at 55 °C).^{10,11} Reddy et al.³² did not observe significant variation for chlorine isotope fractionation associated with alkaline dehydrochlorination of 1,1,1-trichloro-2,2-bis(4-chlorophenyl)ethane (DDT) in a range of temperatures from 52 to 72 °C, revealing no observable temperature dependence. Reaction glass bottles contained 115 mL of aqueous solution and 6 mL of headspace to avoid cracking of the bottles in the thermostatic water bath. Control bottles were prepared like the reactors and stored at 4 °C.

Batch Experiments with Fe(0). Microsized iron powder (<212 μm) was precleaned with acid as described in previous studies.^{16,36} Reactors containing 1 g of Fe(0), 112 mL of aqueous solution and 6 mL of headspace were agitated on an orbital shaker at 200 rpm throughout the course of reaction in order to enable rapid mass transfer of dissolved 1,1,1-TCA to the gas and solid phases. Control bottles without Fe(0) were prepared, sampled and stored in the same way as the reactors.

Concentration and Isotopic Analysis. *Concentration Measurements.* Detailed descriptions of analytical methods as well as details on reaction kinetics calculation are available in the Supporting Information. Briefly, liquid samples were collected for the analysis of 1,1,1-TCA, 1,1-DCE and 1,1-DCA and measured by GC–MS. For the experiments with Fe(0), gas samples from reactors headspace were collected for the analysis of ethene and ethane and measured by GC–flame ionization detection (FID). The average concentration of 1,1,1-TCA in the controls remained equal to the initial concentration within the uncertainty (see the Supporting Information), which indicates that compound losses through the valves and caps during reactors shaking and samples preservation were insignificant. Finally, concentrations of Ac and Cl⁻ were determined by ion chromatography.

Carbon and Chlorine Isotopes Analysis. Carbon isotope ratios (i.e., $^{13}\text{C}/^{12}\text{C}$) of 1,1,1-TCA and daughter products (1,1-DCE, 1,1-DCA, ethene and ethane) were determined by GC–IRMS (see details in the Supporting Information). Chlorine isotope ratios (i.e., $^{37}\text{Cl}/^{35}\text{Cl}$) of 1,1,1-TCA were measured by GC–qMS based on the two most abundant fragment ions (97, 99 m/z). These ions correspond to an isotopologue pair ($[\text{}^{35}\text{Cl}_2\text{}^{12}\text{C}_2\text{}^1\text{H}_3]^+$ and $[\text{}^{35}\text{Cl}^{37}\text{Cl}^{12}\text{C}_2\text{}^1\text{H}_3]^+$, respectively) that differ by one heavy chlorine isotope. The isotope ratio was obtained from the ratio of these isotopologues using eq 1⁵³

$$R = \frac{^{37}\text{Cl}}{^{35}\text{Cl}} = \frac{^{37}p}{^{35}p} = \frac{k}{(n-k+1)} \cdot \frac{^{37}\text{Cl}_{(k)}\text{}^{35}\text{Cl}_{(n-k)}}{^{37}\text{Cl}_{(k-1)}\text{}^{35}\text{Cl}_{(n-k+1)}} = \frac{1}{2} \cdot \frac{^{99}I}{^{97}I} \quad (1)$$

where ^{37}p and ^{35}p are the probabilities of encountering ^{37}Cl and ^{35}Cl , n is the number of Cl atoms, k is the number of ^{37}Cl isotopes, $^{37}\text{Cl}_{(k)}\text{}^{35}\text{Cl}_{(n-k)}$ and $^{37}\text{Cl}_{(k-1)}\text{}^{35}\text{Cl}_{(n-k+1)}$ represent the isotopologues containing k and $(k-1)$ heavy isotopes, respectively, and I indicates the ion peak intensities. Isotope ratios of individual compounds were reported using the delta notation (eq 2)

$$\delta^{\text{hE}}E_{\text{sample}} = \frac{R(\text{}^{\text{hE}}/\text{}^{\text{lE}})_{\text{sample}}}{R(\text{}^{\text{hE}}/\text{}^{\text{lE}})_{\text{standard}}} - 1 \quad (2)$$

where R is the isotope ratio of heavy ($^{\text{hE}}$) and light ($^{\text{lE}}$) isotopes of element E (e.g., $^{13}\text{C}/^{12}\text{C}$ and $^{37}\text{Cl}/^{35}\text{Cl}$). For chlorine, the raw $\delta^{37}\text{Cl}$ values were obtained by referencing against an external laboratory 1,1,1-TCA standard according to eq 2. This standard was dissolved in water and measured like the samples interspersed in the same sequence.⁴¹ Samples and standards were diluted to a similar concentration and each of them was measured ten times. Further details about samples and standards analysis scheme as well as raw $\delta^{37}\text{Cl}$ values (two-point) calibration to the standard mean ocean chloride (SMOC) scale are available in the Supporting Information. Precision (1σ) of the analysis was 0.3‰ (except for ethane, 0.5‰) for $\delta^{13}\text{C}$ and 0.4‰ for $\delta^{37}\text{Cl}$.

Evaluation of 1,1,1-TCA Isotope Fractionation (ϵ_{bulk}). The ϵ_{bulk} value expresses by how much $^{\text{hE}}/\text{}^{\text{lE}}$ is smaller (negative values) or larger (positive values) in the average of freshly formed products compared to the substrate from which they are formed. Calculation of product carbon isotope fractionation trends and substrate AKIEs is indicated in the Supporting Information. Compound-average ϵ_{bulk} values can be calculated using a modified form of the Rayleigh distillation equation:

$$\ln \frac{R_t}{R_0} = \ln \left(\frac{\delta^{\text{hE}}_t + 1}{\delta^{\text{hE}}_0 + 1} \right) = \epsilon_{\text{bulk}} \cdot \ln f \quad (3)$$

where R_t and R_0 are the current and initial isotope ratios, respectively, and f is the remaining fraction of the compound. This equation can also be applied to calculate the isotopic fractionation of chlorine despite the higher natural abundance of ^{37}Cl compared to ^{13}C .⁵³ The ϵ_{bulk} values were quantified by least-squares linear regression of eq 3, without forcing the regression to the origin,⁵⁴ and the uncertainty corresponds to the 95% confidence interval (C.I.) derived from the standard deviation of the regression slope (Figure S1, Supporting Information).

RESULTS AND DISCUSSION

Concentration Patterns and Reaction Kinetics. The 1,1,1-TCA transformation extent was $\geq 90\%$ in all experiments (Figure 1). Degradation of 1,1,1-TCA by activated PS lasted approximately 7 h ($t_{1/2} = 1.5$ h). Neither products nor intermediates were detected by headspace GC/MS analysis (mass scan range 50–300 m/z) performed during the course of reaction. In addition, the good agreement between measured and expected Cl⁻ concentrations (assuming complete dechlorination), indicated that formation of chlorinated products was probably insignificant (Figure 1). Experiments of HY/DH lasted 37 days ($t_{1/2} = 8.0$ d) and 1,1,1-TCA was transformed to 1,1-DCE (yield of $\sim 27\%$, see the Supporting Information) and Ac in parallel reactions. Finally, experiments with Fe(0) lasted 29 h (apparent $t_{1/2} = 9.9$ h) and yielded 1,1-DCA via hydrogenolysis. Nonchlorinated products such as C₄ compounds (from radical coupling reaction) and ethane/ethene (α -elimination) have also been identified in agreement with previous studies.^{14,16,18,19} Concentration patterns of 1,1-DCA, ethene and ethane (Figure 1) agreed well with their formation in parallel reactions (Scheme 1b).^{16,18} A previous reaction study indicated that reduction of ethene by Fe(0) was too slow to

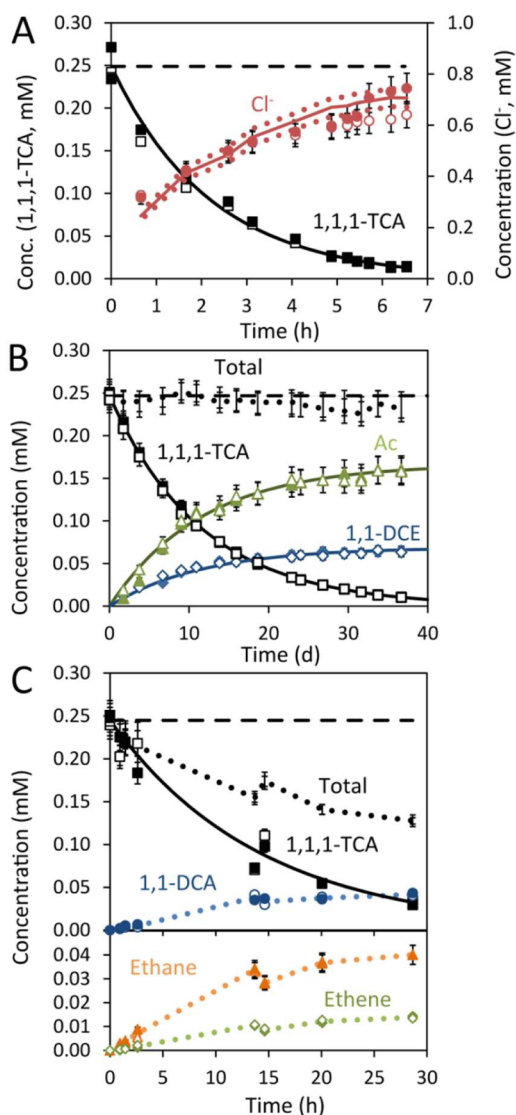


Figure 1. Concentration of 1,1,1-TCA and target products for (A) reaction with PS, (B) HY/DH and (C) reduction by Fe(0) experiments. Data from duplicate experiments were combined (i.e., filled and empty symbols). The total (error bars without symbol marks in panels B and C), the average 1,1,1-TCA concentration in the controls (---, see values in the Supporting Information) and the pseudo-first-order fitting of 1,1,1-TCA, 1,1-DCE and Ac concentration data (—, eqs S1–S3, Supporting Information) are indicated. In panel A, the average (—) and the range (dotted lines) of theoretical Cl^- concentrations from duplicate experiments are shown. Error bars correspond to the total relative uncertainties of $\leq 8\%$ (for 1,1,1-TCA, 1,1-DCE and 1,1-DCA), $\leq 10\%$ (for ethene and ethane) and 8% (for Ac and Cl^-). In some cases, error bars are smaller than the symbols.

account for the amount of produced ethane and postulated that ethene could be formed through rearrangement of $\text{H}_3\text{C}-\dot{\text{C}}-\text{H}$ carbenoid (a four electron reduction intermediate of 1,1,1-TCA transformation to ethane) (Scheme S1, Supporting Information).¹⁶ Final concentrations of 1,1-DCA, ethene, ethane and remaining 1,1,1-TCA reflected a mass balance deficit of approximately 48% (i.e., mass amount necessary to maintain the system mass balance expressed as percent of the initial mass). A high deficit was previously observed for 1,1,1-TCA reduction by FeS (79%⁵⁵ and $\sim 94\%$ ^{14,56}) or bimetallic reductants (up to $\sim 20\%$ ^{16,19}). The detected but not quantified

C_4 , C_5 and C_6 species could explain the unclosed mass balance in our study. In addition to C_4 – C_6 compounds, acetaldehyde^{57,58} could be a potential product but was not analyzed in our study.

Chlorine Isotope Patterns of 1,1,1-TCA. The $\delta^{37}\text{Cl}$ of 1,1,1-TCA showed a trend to more positive values during its transformation by HY/DH or Fe(0) (Figure 2), which reflects an enrichment of 1,1,1-TCA in a heavy isotope (^{37}Cl , eq 2), indicative of a normal isotope effect. In contrast, for reaction of 1,1,1-TCA with PS, a constant $\delta^{37}\text{Cl}$ was observed. For HY/DH and Fe(0) pathways, chlorine isotope data followed a Rayleigh trend ($r^2 = 0.997$, eq 3, Figure S1, Supporting Information) and resultant $\epsilon_{\text{bulk}}^{\text{Cl}}$ values were in a similar range, -4.7 ± 0.1 and $-5.2 \pm 0.2\%$ for HY/DH and Fe(0), respectively (Figure 2).

Carbon Isotope Patterns for Substrate and Products. For all reactions investigated, an enrichment of 1,1,1-TCA in ^{13}C was observed, indicative of a normal isotope effect (Figure 2). The $\delta^{13}\text{C}$ of 1,1,1-TCA in the controls of all experiments ($-26.5 \pm 0.3\%$) did not change significantly from the initial value ($\delta^{13}\text{C}_0 = -26.3 \pm 0.1\%$). The carbon isotope composition of 1,1,1-TCA followed a Rayleigh trend ($r^2 \geq 0.96$, eq 3, Figure S1, Supporting Information) with $\epsilon_{\text{bulk}}^{\text{C}}$ values ranging from -1.6% (HY/DH) to -7.8% (Fe(0)) (Figure 2). The products analyzed were initially depleted in ^{13}C compared to the initial value of the substrate, in agreement with the normal isotope effect. The $\delta^{13}\text{C}$ of the products also shifted toward more positive values during the course of reaction reflecting the substrate enrichment in ^{13}C (Figure 2).

For reaction with heat-activated PS, an $\epsilon_{\text{bulk}}^{\text{C}}$ of $-4.0 \pm 0.2\%$ was determined (Figure 2) but no products were recovered for isotope analysis. The obtained carbon isotope enrichment factor was smaller than the one reported for base-activated PS reaction ($\epsilon_{\text{bulk}}^{\text{C}} = -7.0 \pm 0.2\%$) in a recent study.²¹ For HY/DH, the relatively small $\epsilon_{\text{bulk}}^{\text{C}}$ of $-1.6 \pm 0.2\%$ was consistent with the small depletion in ^{13}C observed for 1,1-DCE. The largest carbon isotope enrichment factor ($\epsilon_{\text{bulk}}^{\text{C}} = -7.8 \pm 0.4\%$) was obtained for reduction by Fe(0), which agreed with the stronger depletion in ^{13}C of some of the products (Figure 2). The α -elimination products (ethene and ethane) showed a similar depletion in ^{13}C relative to the substrate, but a much larger depletion in ^{13}C was observed for the hydrogenolysis product (1,1-DCA). The observed isotope pattern with constant discrimination between products was indicative of product formation in parallel pathways. In addition, the significant isotope discrimination between hydrogenolysis and α -elimination products (about 9% , Figure 2E) was consistent with the formation of a common radical intermediate in the first reaction step (Scheme 1b). The reason is that different bonds are broken or formed in subsequent reactions of the common intermediate (Scheme S1, Supporting Information), which are likely associated with different isotope effects. Interestingly, the product isotope pattern for 1,1,1-TCA is different than that observed during reduction of TCE by Fe(0) in previous studies.^{46,59} Contrary to reduction of 1,1,1-TCA, ethene/ethane produced from TCE were constantly depleted in ^{13}C (about 10%) compared to the hydrogenolysis product (*cis*-dichloroethylene). The difference between the product isotope patterns of TCE and 1,1,1-TCA could be due to distinct reaction mechanisms leading to formation of ethene/ethane. The occurrence of distinct mechanisms is supported by previous studies indicating that production of ethene/ethane

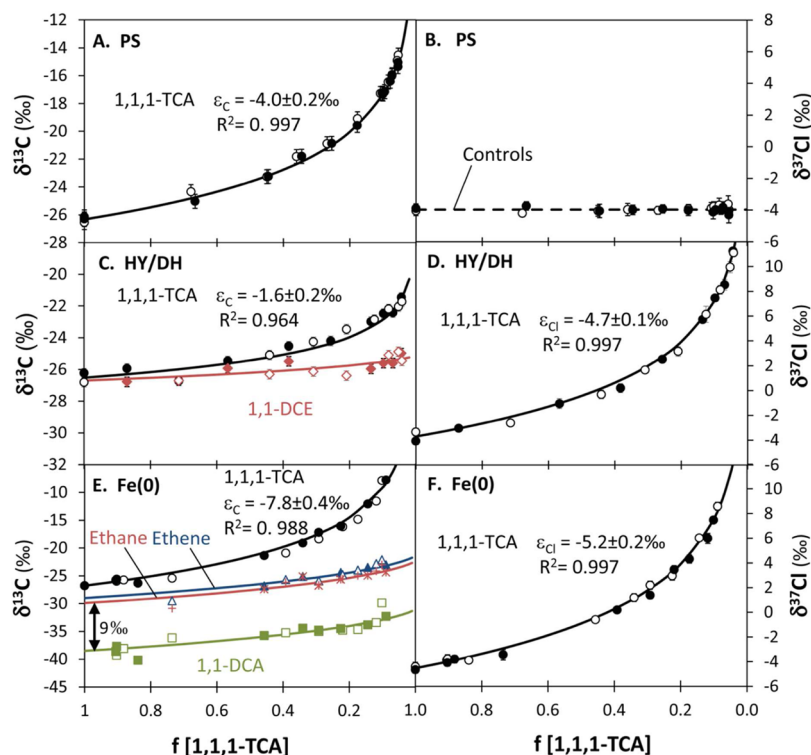


Figure 2. Isotopic composition of the substrate ($\delta^{13}\text{C}$ and $\delta^{37}\text{Cl}$) and products ($\delta^{13}\text{C}$) for reaction of 1,1,1-TCA with PS (A, B), HY/DH (C, D) and reduction by Fe(0) (E, F). Data from duplicate experiments were combined and symbols are as follows: 1,1,1-TCA (circles), 1,1-DCE (diamonds), 1,1-DCA (squares), ethene (triangles) and ethane (crosses). The uncertainty of ϵ_{bulk} values corresponds to the 95% confidence interval. The average $\delta^{37}\text{Cl}$ of 1,1,1-TCA in the controls (---, panel B) and models fit (—) to isotope data from the substrate (eq 3) and products (eq S4, Supporting Information) are shown.

from TCE mainly proceeds via β -dichloroelimination to chloroacetylene.^{46,60}

For the Fe(0) pathway, an $\epsilon_{\text{bulk}}^{\text{C}}$ of $-13.6 \pm 0.5\%$ from a previous study is available for comparison.³⁶ This value is larger than the one determined in our study ($-7.8 \pm 0.4\%$), however, significant variation ranging from -10.3 to -14.0% has also been recently observed during reduction of 1,1,1-TCA by biotically mediated FeS formation in microcosm experiments.¹⁵ Similarly, high variability of $\epsilon_{\text{bulk}}^{\text{C}}$ has been reported for reductive dechlorination of chlorinated ethenes by Fe(0). For instance, a range from -6.9 to -20.1% has been observed for vinyl chloride (VC) where, in contrast to polychlorinated ethenes, only hydrogenolysis is possible (see ref⁴⁶ and references herein). Such variability could be explained by the presence of preceding rate-limiting steps.⁶¹ If dehalogenation (isotope fractionating step) becomes fast due to a high reactivity of the metal or substrate, preceding steps such as the formation of organohalide-metal complexes may become rate-limiting. In this case, if preceding (rate-limiting) steps exhibit small or no isotope fractionation, the observable isotope effect will be smaller (i.e., masked) than the intrinsic isotope effect.^{30,61}

It is important to note that for cleavage of a C–Cl bond, primary isotope effects for carbon are generally expected to be higher than for chlorine because carbon has a larger relative mass difference between its heavy and light isotopes (i.e., 8.3% mass difference between $m^{12}\text{C} = 12$ and $m^{13}\text{C} = 13$ versus 5.7% mass difference between $m^{35}\text{Cl} = 35$ and $m^{37}\text{Cl} = 37$, relative to the mass of the respective light isotope).⁴⁹ However, for reasons discussed in more detail below, for HY/DH the isotope fractionation for chlorine ($-4.7 \pm 0.1\%$) was unexpectedly

larger than for carbon ($-1.6 \pm 0.2\%$), and in a similar range for reduction by Fe(0) (-5.2 ± 0.2 and $-7.8 \pm 0.4\%$, respectively).

Dual C–Cl Isotope Approach to Differentiate Degradation Pathways. Carbon and chlorine δ isotope values of 1,1,1-TCA from the three investigated reaction pathways were compared in a dual isotope plot. All reactions showed linear trends with strongly different slopes (Figure 3). For reaction with PS, a vertical trend was obtained due to the absence of chlorine isotope fractionation; whereas for HY/DH and Fe(0) reactions, different slopes ($\Lambda = \Delta\delta^{13}\text{C}/\Delta\delta^{37}\text{Cl} \approx \epsilon_{\text{bulk}}^{\text{C}}/\epsilon_{\text{bulk}}^{\text{Cl}}$) were observed as a result of the difference in their $\epsilon_{\text{bulk}}^{\text{C}}$ values (-1.6 ± 0.2 and $-7.8 \pm 0.4\%$, respectively) compared to the similar $\epsilon_{\text{bulk}}^{\text{Cl}}$ (-4.7 ± 0.1 and $-5.2 \pm 0.2\%$, respectively). The clearly distinct dual C–Cl isotope trends for the three reactions opens the possibility of a dual isotope approach to identify the different abiotic degradation pathways of 1,1,1-TCA in the field. The large difference between trends also enables to estimate the proportion of two competing pathways based on the resultant slope,^{62,63} assuming simultaneous activity with a constant ratio between both pathway rates. Even if $\epsilon_{\text{bulk}}^{\text{C}}$ values are significantly different for distinct reactions, a single element approach is not sufficient to distinguish degradation pathways under field conditions. The reason is that a certain extent of observable carbon isotope fractionation in the field (i.e. $\Delta\delta^{13}\text{C}$) could have been caused by a strongly isotope fractionating reaction that has proceeded little, or a weakly isotope fractionating reaction that has proceeded further. Only the analysis of a second element was possible to resolve this issue.

Mechanistic Insights. The dual isotope trend observed for reaction of 1,1,1-TCA with PS, with constant $\delta^{37}\text{Cl}$ values,

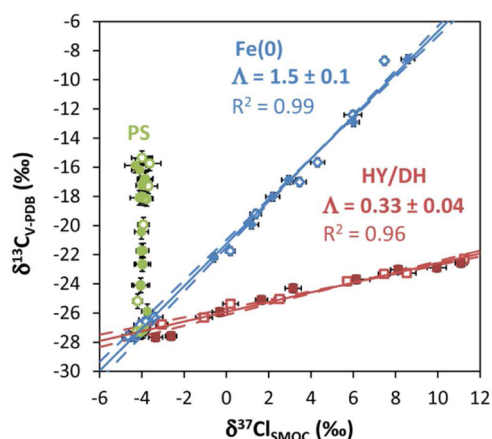


Figure 3. Dual C–Cl isotope plots during transformation of 1,1,1-TCA in the investigated experimental systems. Data from duplicate experiments were combined, i.e., empty and filled symbols: red squares for HY/DH, blue rhombus for reduction by Fe(0) and green circles for reaction with PS. Λ values ($\pm 95\%$ C.I.) are given by the slope of the linear regressions (—) and the lines (---) correspond to the 95% C.I.

suggests that no cleavage of C–Cl occurs at the first reaction step. This result provides a direct evidence of oxidative C–H bond cleavage in the first reaction step (Scheme 1c), confirming 1,1,1-TCA degradation via H abstraction as proposed by a recent reaction study.²⁵ The calculated ^{13}C -AKIE in our study (1.0081 ± 0.0002 , Table S2, Supporting Information) was also consistent with the typical ^{13}C -KIE for oxidative C–H bond cleavage (1.01–1.03).⁴⁹ The difference between the $\epsilon_{\text{bulk}}^{\text{C}}$ value determined in our study ($-4.0 \pm 0.2\%$) and the value obtained for 1,1,1-TCA reaction with base-activated PS ($-7.0 \pm 0.2\%$)²¹ might be due to different underlying reaction mechanisms. However, conclusions cannot be drawn, as only carbon isotope ratios were measured in the previous study with base-activated PS,²¹ highlighting the benefit of using a dual C–Cl isotope approach.

For the HY/DH and Fe(0) reaction pathways, distinctly different slopes were obtained, although both pathways involve cleavage of a C–Cl bond in their initial reaction step (Scheme 1a,b). To address this question, a closer look at the two pathways is necessary. For HY/DH, the reaction could proceed via formation of a common carbocation intermediate (^{13}C -AKIE = 1.0033 ± 0.0004 , Table S2, Supporting Information) or via two parallel reactions starting from the substrate ($\text{S}_{\text{N}}2$ vs $\text{E}2$ mechanisms). If the latter case was true, the $\text{S}_{\text{N}}2$ reaction would dominate the isotope fractionation of the substrate according with the product distribution (the yield of the Ac by nucleophilic substitution was approximately 73%, Figure 1). However, considering the usually large ^{13}C -KIE associated with $\text{S}_{\text{N}}2$ reaction (typical range from 1.03 to 1.09),⁴⁹ this mechanism is less plausible compared to a $\text{S}_{\text{N}}1$ (typical range from 1.00 to 1.03)⁴⁹ (see the Supporting Information). Degradation of 1,1,1-TCA via formation of a common carbocation intermediate is supported by previous reaction studies^{11,13} showing that variation of reaction conditions (i.e., T and pH) did not cause significant changes in the product distribution and transformation rate, respectively. Variation of reaction conditions as a means to induce changes in the product distribution is a commonly used approach to obtain insight about branching points. However, as it can be difficult to observe significant variation of the product ratio with varying

reaction conditions, sometimes it is not possible to draw sound conclusions using this approach.^{12,64} Therefore, the isotope results show that complementary evidence could be obtained by comparing determined AKIEs with expected KIEs (see the Supporting Information). The resultant chlorine isotope effect was large (^{37}Cl -AKIE = 1.0145 ± 0.0003) relative to the carbon (^{13}C -AKIE = 1.0033 ± 0.0004), which is not expected if isotope fractionation was caused only by primary isotope effects associated with cleavage of a C–Cl bond (see above). Apparent KIEs (Table S2, Supporting Information) were calculated assuming that the first (isotope fractionating) step was only associated with primary isotope effects and,⁴⁹ therefore, α -secondary ^{37}Cl -KIEs are very likely to contribute. Similarly, for reduction by Fe(0), estimated AKIEs for C–Cl bond cleavage by SET exhibited similar values, 1.0158 ± 0.0008 (^{13}C -AKIE) and 1.0160 ± 0.0006 (^{37}Cl -AKIE), suggesting that α -secondary chlorine isotope effects also play a role. In summary, different magnitudes of secondary chlorine isotope effects associated with the HY/DH and Fe(0) reaction mechanisms could at least be partly responsible for the different dual C–Cl isotope slopes. The occurrence of α -secondary ^{37}Cl -KIEs is supported by significant secondary chlorine isotope effects measured experimentally during 1,2-dichloroethane (1,2-DCA) aerobic biodegradation in a recent study.³⁷

Environmental Significance. Subsurface contamination by chlorinated ethanes is one of the major ecological problems, and the assessment of their fate in groundwater is a complex task. The distinctly different dual isotope trends shows the feasibility of this approach for 1,1,1-TCA abiotic degradation pathways differentiation in the field (Figure 3). The large difference of slopes (Λ) between the abiotic reductive (Fe(0)) and oxidative (PS) pathways suggest that aerobic and anaerobic biodegradation of 1,1,1-TCA could be also differentiated using this approach, provided that these different isotope trends can be confirmed in future biodegradation studies. Aerobic and anaerobic biotransformation of 1,1,1-TCA to 2,2,2-trichloroethanol (via C–H bond oxidation)^{65,66} and to 1,1-DCA (via C–Cl bond cleavage),⁶ respectively, has been well documented in previous studies.

In addition, the product carbon isotope pattern obtained for 1,1,1-TCA reduction by Fe(0) could be used to distinguish between biotic and abiotic reductive dechlorination. While biotic sequential reductive dechlorination (i.e., 1,1,1-TCA \rightarrow 1,1-DCA \rightarrow CA \rightarrow ethane) would produce ethane initially depleted in ^{13}C relative to 1,1-DCA, the opposite was observed for reaction with Fe(0). However, although biodegradation of CA to ethane has been reported,⁶⁷ there is currently a lack of comprehensive experimental evidence for complete anaerobic dechlorination of 1,1,1-TCA via hydrogenolysis.³

One of the main applications of CSIA to field studies is the estimation of contaminant degradation extent using the Rayleigh equation.^{68,69} For this purpose, knowledge of the 1,1,1-TCA degradation pathway at the site and its corresponding $\epsilon_{\text{bulk}}^{\text{C}}$ and/or $\epsilon_{\text{bulk}}^{\text{Cl}}$ values are necessary. However, in contrast to chlorinated ethenes, reported ϵ_{bulk} values for chlorinated ethanes are scarce in the literature. The new isotope fractionation values of 1,1,1-TCA determined for HY/DH, oxidation by heat-activated PS (both $\epsilon_{\text{bulk}}^{\text{C}}$ and $\epsilon_{\text{bulk}}^{\text{Cl}}$) and reduction by Fe(0) ($\epsilon_{\text{bulk}}^{\text{Cl}}$) increase the possibility of using CSIA in sites polluted by 1,1,1-TCA. In addition, higher absolute ϵ_{bulk} values lead to estimates with a minor uncertainty⁶⁸ and, therefore, for HY/DH chlorine isotope ratios ($\epsilon_{\text{bulk}}^{\text{Cl}} = -4.7 \pm 0.1\%$) could be used instead of carbon ($\epsilon_{\text{bulk}}^{\text{C}} = -1.6 \pm 0.2\%$)

to assess 1,1,1-TCA transformation in the field. This study demonstrates that abiotic 1,1,1-TCA transformation processes can unambiguously be identified and evaluated using a dual C–Cl isotope approach.

■ AUTHOR INFORMATION

Corresponding Author

*Jordi Palau. Address: Centre d'Hydrogéologie et de Géothermie, Université de Neuchâtel, Rue Emile-Argand 11, CH-2000 Neuchâtel, Switzerland. E-mail: jordi.palau@ub.edu.

Author Contributions

The paper was written through contributions of all authors. All authors have given approval to the final version of the paper.

Notes

The authors declare no competing financial interest.

■ ACKNOWLEDGMENTS

We thank four anonymous reviewers for their helpful comments and suggestions that improved the quality of the paper. We are grateful to B. Schlunegger for her help in the laboratory. The research was supported by the University of Neuchâtel via direct university funding.

■ REFERENCES

- (1) Squillace, P. J.; Moran, M. J.; Lapham, W. W.; Price, C. V.; Clawges, R. M.; Zogorski, J. S. Volatile organic compounds in untreated ambient groundwater of the United States, 1985–1995. *Environ. Sci. Technol.* **1999**, *33* (23), 4176–4187.
- (2) ATDSR. Toxicological profile for 1,1,1-trichloroethane. <http://www.atsdr.cdc.gov/tfacts70.pdf> (accessed January 7, 2014).
- (3) Scheutz, C.; Durant, N. D.; Hansen, M. H.; Bjerg, P. L. Natural and enhanced anaerobic degradation of 1,1,1-trichloroethane and its degradation products in the subsurface - A critical review. *Water Res.* **2011**, *45* (9), 2701–2723.
- (4) Tobiszewski, M.; Namiesnik, J. Abiotic degradation of chlorinated ethanes and ethenes in water. *Environ. Sci. Pollut. Res.* **2012**, *19* (6), 1994–2006.
- (5) O'Loughlin, E. J.; Burris, D. R. Reduction of halogenated ethanes by green rust. *Environ. Toxicol. Chem.* **2004**, *23* (1), 41–48.
- (6) Sun, B. L.; Griffin, B. M.; Ayala-del-Rio, H. L.; Hashsham, S. A.; Tiedje, J. M. Microbial dehalorespiration with 1,1,1-trichloroethane. *Science* **2002**, *298* (5595), 1023–1025.
- (7) Grostern, A.; Edwards, E. A. A 1,1,1-trichloroethane-degrading anaerobic mixed microbial culture enhances biotransformation of mixtures of chlorinated ethenes and ethanes. *Appl. Environ. Microbiol.* **2006**, *72* (12), 7849–7856.
- (8) Scheutz, C.; Durant, N. D.; Broholm, M. M. Effects of bioaugmentation on enhanced reductive dechlorination of 1,1,1-trichloroethane in groundwater: A comparison of three sites. *Biodegradation* **2014**, *25* (3), 459–478.
- (9) USEPA. Priority pollutants. <http://water.epa.gov/scitech/methods/cwa/pollutants.cfm> (accessed January 7, 2014).
- (10) Gerken, R. R.; Franklin, J. A. The rate of degradation of 1,1,1-trichloroethane in water by hydrolysis and dehydrochlorination. *Chemosphere* **1989**, *19* (12), 1929–1937.
- (11) Jeffers, P. M.; Ward, L. M.; Woytowitch, L. M.; Wolfe, N. L. Homogeneous hydrolysis rate constants for selected chlorinated methanes, ethanes, ethenes, and propanes. *Environ. Sci. Technol.* **1989**, *23* (8), 965–969.
- (12) Schwarzenbach, R. P. G.; Gschwend, P. M.; Imboden, D. M. *Environmental Organic Chemistry*, Second ed.; John Wiley & Sons, Inc.: Hoboken, NJ, 2003; p 1313.
- (13) Haag, W. R.; Mill, T. Effect of a subsurface sediment on hydrolysis of haloalkanes and epoxides. *Environ. Sci. Technol.* **1988**, *22* (6), 658–663.
- (14) Gander, J. W.; Parkin, G. F.; Scherer, M. M. Kinetics of 1,1,1-trichloroethane transformation by iron sulfide and a methanogenic consortium. *Environ. Sci. Technol.* **2002**, *36* (21), 4540–4546.
- (15) Broholm, M. M.; Hunkeler, D.; Tuxen, N.; Jeannotat, S.; Scheutz, C. Stable carbon isotope analysis to distinguish biotic and abiotic degradation of 1,1,1-trichloroethane in groundwater sediments. *Chemosphere* **2014**, 265–273.
- (16) Fennelly, J. P.; Roberts, A. L. Reaction of 1,1,1-trichloroethane with zero-valent metals and bimetallic reductants. *Environ. Sci. Technol.* **1998**, *32* (13), 1980–1988.
- (17) Lookman, R.; Bastiaens, L.; Borremans, B.; Maesen, M.; Gemoets, J.; Diels, L. Batch-test study on the dechlorination of 1,1,1-trichloroethane in contaminated aquifer material by zero-valent iron. *J. Contam. Hydrol.* **2004**, *74* (1–4), 133–144.
- (18) Song, H.; Carraway, E. R. Reduction of chlorinated ethanes by nanosized zero-valent iron: Kinetics, pathways, and effects of reaction conditions. *Environ. Sci. Technol.* **2005**, *39* (16), 6237–6245.
- (19) Cwiertny, D. M.; Bransfield, S. J.; Livi, K. J. T.; Fairbrother, D. H.; Roberts, A. L. Exploring the influence of granular iron additives on 1,1,1-trichloroethane reduction. *Environ. Sci. Technol.* **2006**, *40* (21), 6837–6843.
- (20) Wu, X. L.; Lu, S. G.; Qiu, Z. F.; Sui, Q.; Lin, K. F.; Du, X. M.; Luo, Q. S. The reductive degradation of 1,1,1-trichloroethane by Fe(0) in a soil slurry system. *Environ. Sci. Pollut. Res.* **2014**, *21* (2), 1401–1410.
- (21) Marchesi, M.; Thomson, N. R.; Aravena, R.; Sra, K. S.; Otero, N.; Soler, A. Carbon isotope fractionation of 1,1,1-trichloroethane during base-catalyzed persulfate treatment. *J. Hazard. Mater.* **2013**, *260*, 61–66.
- (22) Liang, C. J.; Bruell, C. J.; Marley, M. C.; Sperry, K. L. Thermally activated persulfate oxidation of trichloroethylene (TCE) and 1,1,1-trichloroethane (TCA) in aqueous systems and soil slurries. *Soil Sediment Contam.* **2003**, *12* (2), 207–228.
- (23) Huang, K. C.; Zhao, Z. Q.; Hoag, G. E.; Dahmani, A.; Block, P. A. Degradation of volatile organic compounds with thermally activated persulfate oxidation. *Chemosphere* **2005**, *61* (4), 551–560.
- (24) Gu, X. G.; Lu, S. G.; Li, L.; Qiu, Z. F.; Sui, Q.; Lin, K. F.; Luo, Q. S. Oxidation of 1,1,1-trichloroethane stimulated by thermally activated persulfate. *Ind. Eng. Chem. Res.* **2011**, *50* (19), 11029–11036.
- (25) Xu, M. H.; Gu, X. G.; Lu, S. G.; Qiu, Z. F.; Sui, Q. Role of reactive oxygen species for 1,1,1-trichloroethane degradation in a thermally activated persulfate system. *Ind. Eng. Chem. Res.* **2014**, *53* (3), 1056–1063.
- (26) Waldemer, R. H.; Tratnyek, P. G.; Johnson, R. L.; Nurmi, J. T. Oxidation of chlorinated ethenes by heat-activated persulfate: Kinetics and products. *Environ. Sci. Technol.* **2007**, *41* (3), 1010–5.
- (27) Furman, O. S.; Teel, A. L.; Watts, R. J. Mechanism of base activation of persulfate. *Environ. Sci. Technol.* **2010**, *44* (16), 6423–6428.
- (28) Velimirovic, M.; Simons, Q.; Bastiaens, L. Guar gum coupled microscale ZVI for in situ treatment of CAHs: Continuous-flow column study. *J. Hazard. Mater.* **2014**, *265*, 20–29.
- (29) Suthersan, S.; Horst, J.; Klemmer, M.; Malone, D. Temperature-activated auto-decomposition reactions: An under-utilized in situ remediation solution. *Ground Water Monit. Rev.* **2012**, *32* (3), 34–40.

- (30) Elsner, M. Stable isotope fractionation to investigate natural transformation mechanisms of organic contaminants: Principles, prospects and limitations. *J. Environ. Monit.* **2010**, *12* (11), 2005–2031.
- (31) Hofstetter, T. B.; Berg, M. Assessing transformation processes of organic contaminants by compound-specific stable isotope analysis. *TrAC, Trends Anal. Chem.* **2011**, *30* (4), 618–627.
- (32) Hofstetter, T. B.; Schwarzenbach, R. P.; Bernasconi, S. M. Assessing transformation processes of organic compounds using stable isotope fractionation. *Environ. Sci. Technol.* **2008**, *42* (21), 7737–7743.
- (33) Hofstetter, T. B.; Bolotin, J.; Skarpeli-Liati, M.; Wijk, R.; Kurt, Z.; Nishino, S. F.; Spain, J. C. Tracking transformation processes of organic micropollutants in aquatic environments using multi-element isotope fractionation analysis. *Appl. Geochem.* **2011**, *26*, S334–S336.
- (34) Zwank, L.; Berg, M.; Elsner, M.; Schmidt, T. C.; Schwarzenbach, R. P.; Haderlein, S. B. New evaluation scheme for two-dimensional isotope analysis to decipher biodegradation processes: Application to groundwater contamination by MTBE. *Environ. Sci. Technol.* **2005**, *39* (4), 1018–1029.
- (35) Braeckvelt, M.; Fischer, A.; Kastner, M. Field applicability of compound-specific isotope analysis (CSIA) for characterization and quantification of in situ contaminant degradation in aquifers. *Appl. Microbiol. Biotechnol.* **2012**, *94* (6), 1401–1421.
- (36) Elsner, M.; Cwiertny, D. M.; Roberts, A. L.; Lollar, B. S. 1,1,2,2-Tetrachloroethane reactions with OH⁻, Cr(II), granular iron, and a copper-iron bimetal: Insights from product formation and associated carbon isotope fractionation. *Environ. Sci. Technol.* **2007**, *41* (11), 4111–4117.
- (37) Palau, J.; Cretnik, S.; Shouakar-Stash, O.; Hoche, M.; Elsner, M.; Hunkeler, D. C and Cl isotope fractionation of 1,2-dichloroethane displays unique delta(13)C/delta(37)Cl Patterns for pathway identification and reveals surprising C-Cl bond involvement in microbial oxidation. *Environ. Sci. Technol.* **2014**, *48* (16), 9430–7.
- (38) Shouakar-Stash, O.; Drimmie, R. J.; Zhang, M.; Frape, S. K. Compound-specific chlorine isotope ratios of TCE, PCE and DCE isomers by direct injection using CF-IRMS. *Appl. Geochem.* **2006**, *21* (5), 766–781.
- (39) Sakaguchi-Soder, K.; Jager, J.; Grund, H.; Matthaus, F.; Schuth, C. Monitoring and evaluation of dechlorination processes using compound-specific chlorine isotope analysis. *Rapid Commun. Mass Spectrom.* **2007**, *21* (18), 3077–3084.
- (40) Jin, B.; Laskov, C.; Rolle, M.; Haderlein, S. B. Chlorine isotope analysis of organic contaminants using GC-qMS: Method optimization and comparison of different evaluation schemes. *Environ. Sci. Technol.* **2011**, *45* (12), 5279–86.
- (41) Aeppli, C.; Holmstrand, H.; Andersson, P.; Gustafsson, O. Direct compound-specific stable chlorine isotope analysis of organic compounds with quadrupole GC/MS using standard isotope bracketing. *Anal. Chem.* **2010**, *82* (1), 420–426.
- (42) Elsner, M.; Jochmann, M. A.; Hofstetter, T. B.; Hunkeler, D.; Bernstein, A.; Schmidt, T. C.; Schimmelmann, A. Current challenges in compound-specific stable isotope analysis of environmental organic contaminants. *Anal. Bioanal. Chem.* **2012**, *403* (9), 2471–2491.
- (43) Cincinelli, A.; Pieri, F.; Zhang, Y.; Seed, M.; Jones, K. C. Compound Specific Isotope Analysis (CSIA) for chlorine and bromine: A review of techniques and applications to elucidate environmental sources and processes. *Environ. Pollut.* **2012**, *169*, 112–127.
- (44) Abe, Y.; Aravena, R.; Zopfi, J.; Shouakar-Stash, O.; Cox, E.; Roberts, J. D.; Hunkeler, D. Carbon and chlorine isotope fractionation during aerobic oxidation and reductive dechlorination of vinyl chloride and cis-1,2-dichloroethene. *Environ. Sci. Technol.* **2009**, *43* (1), 101–107.
- (45) Cretnik, S.; Thoreson, K. A.; Bernstein, A.; Ebert, K.; Buchner, D.; Laskov, C.; Haderlein, S.; Shouakar-Stash, O.; Kliegman, S.; McNeill, K.; Elsner, M. Reductive dechlorination of TCE by chemical model systems in comparison to dehalogenating bacteria: Insights from dual element isotope analysis (¹³C/¹²C, ³⁷Cl/³⁵Cl). *Environ. Sci. Technol.* **2013**, *47* (13), 6855–6863.
- (46) Audí-Miró, C.; Cretnik, S.; Otero, N.; Palau, J.; Shouakar-Stash, O.; Soler, A.; Elsner, M. Cl and C isotope analysis to assess the effectiveness of chlorinated ethene degradation by zero-valent iron: Evidence from dual element and product isotope values. *Appl. Geochem.* **2013**, *32* (0), 175–183.
- (47) Liu, Y.; Gan, Y.; Zhou, A.; Liu, C.; Li, X.; Yu, T. Carbon and chlorine isotope fractionation during Fenton-like degradation of trichloroethene. *Chemosphere* **2014**, *107*, 94–100.
- (48) Lojkasek-Lima, P.; Aravena, R.; Shouakar-Stash, O.; Frape, S. K.; Marchesi, M.; Fiorenza, S.; Vogan, J. Evaluating TCE abiotic and biotic degradation pathways in a permeable reactive barrier using compound specific isotope analysis. *Ground Water Monit. Rev.* **2012**, *32* (4), 53–62.
- (49) Elsner, M.; Zwank, L.; Hunkeler, D.; Schwarzenbach, R. P. A new concept linking observable stable isotope fractionation to transformation pathways of organic pollutants. *Environ. Sci. Technol.* **2005**, *39* (18), 6896–6916.
- (50) Tobler, N. B.; Hofstetter, T. B.; Schwarzenbach, R. P. carbon and hydrogen isotope fractionation during anaerobic toluene oxidation by geobacter metallireducens with different Fe(III) phases as terminal electron acceptors. *Environ. Sci. Technol.* **2008**, *42* (21), 7786–7792.
- (51) Thullner, M.; Fischer, A.; Richnow, H. H.; Wick, L. Y. Influence of mass transfer on stable isotope fractionation. *Appl. Microbiol. Biotechnol.* **2013**, *97* (2), 441–52.
- (52) Reddy, C. M.; Drenzek, N. J.; Eglinton, T. I.; Heraty, L. J.; Sturchio, N. C.; Shiner, V. J. Stable chlorine intramolecular kinetic isotope effects from the abiotic dehydrochlorination of DDT. *Environ. Sci. Pollut. Res.* **2002**, *9* (3), 183–186.
- (53) Elsner, M.; Hunkeler, D. Evaluating chlorine isotope effects from isotope ratios and mass spectra of polychlorinated molecules. *Anal. Chem.* **2008**, *80* (12), 4731–4740.
- (54) Scott, K. M.; Lu, X.; Cavanaugh, C. M.; Liu, J. S. Optimal methods for estimating kinetic isotope effects from different forms of the Rayleigh distillation equation. *Geochim. Cosmochim. Acta* **2004**, *68* (3), 433–442.
- (55) Choi, J.; Choi, K.; Lee, W. Effects of transition metal and sulfide on the reductive dechlorination of carbon tetrachloride and 1,1,1-trichloroethane by FeS. *J. Hazard. Mater.* **2009**, *162* (2–3), 1151–1158.
- (56) Butler, E. C.; Hayes, K. F. Kinetics of the transformation of halogenated aliphatic compounds by iron sulfide. *Environ. Sci. Technol.* **2000**, *34* (3), 422–429.
- (57) Bussan, A. L.; Strathmann, T. J. Influence of organic ligands on the reduction of polyhalogenated alkanes by iron(II). *Environ. Sci. Technol.* **2007**, *41* (19), 6740–6747.
- (58) Castro, C. E.; Kray, W. C. Carbenoid intermediates from polyhalomethanes and chromium(2). Homogeneous reduction of geminal halides by chromous sulfate. *J. Am. Chem. Soc.* **1966**, *88* (19), 4447–8.
- (59) Elsner, M.; Chartrand, M.; Vanstone, N.; Couloume, G. L.; Lollar, B. S. Identifying abiotic chlorinated ethene degradation: Characteristic isotope patterns in reaction products with nanoscale zero-valent iron. *Environ. Sci. Technol.* **2008**, *42* (16), 5963–5970.
- (60) Arnold, W. A.; Roberts, A. L. Pathways and kinetics of chlorinated ethylene and chlorinated acetylene reaction with Fe(O) particles. *Environ. Sci. Technol.* **2000**, *34* (9), 1794–1805.
- (61) Zwank, L.; Elsner, M.; Aeberhard, A.; Schwarzenbach, R. P.; Haderlein, S. B. Carbon isotope fractionation in the reductive dehalogenation of carbon tetrachloride at iron (hydr)oxide and iron sulfide minerals. *Environ. Sci. Technol.* **2005**, *39* (15), 5634–5641.
- (62) van Breukelen, B. M. Extending the Rayleigh equation to allow competing isotope fractionating pathways to improve quantification of biodegradation. *Environ. Sci. Technol.* **2007**, *41* (11), 4004–10.
- (63) Centler, F.; Hesse, F.; Thullner, M. Estimating pathway-specific contributions to biodegradation in aquifers based on dual isotope analysis: Theoretical analysis and reactive transport simulations. *J. Contam. Hydrol.* **2013**, *152*, 97–116.
- (64) Elsner, M.; Hofstetter, T. B. Current perspectives on the mechanisms of chlorohydrocarbon degradation in subsurface environ-

ments: Insight from kinetics, product formation, probe molecules, and isotope fractionation. In *Aquatic Redox Chemistry*; Tratnyek, P. G., Grundl, T. J., Haderlein, S. B., Eds.; ACS Symposium Series; American Chemical Society: Washington, DC, 2011; Vol. 1071, pp 407–439.

(65) Oldenhuis, R.; Vink, R. L. J. M.; Janssen, D. B.; Witholt, B. Degradation of chlorinated aliphatic-hydrocarbons by methylotrichosporium Ob3b expressing soluble methane monoxygenase. *Appl. Environ. Microbiol.* **1989**, *55* (11), 2819–2826.

(66) Hashimoto, A.; Iwasaki, K.; Nakasugi, N.; Nakajima, M.; Yagi, O. Degradation pathways of trichloro ethylene and 1,1,1-trichloroethane by *Mycobacterium* sp TA27. *Biosci. Biotechnol. Biochem.* **2002**, *66* (2), 385–390.

(67) Holliger, C.; Schraa, G.; Stams, A. J. M.; Zehnder, A. J. B. Reductive dechlorination of 1,2-dichloroethane and chloroethane by cell suspensions of methanogenic bacteria. *Biodegradation* **1990**, *1* (4), 253–261.

(68) Thullner, M.; Centler, F.; Richnow, H. H.; Fischer, A. Quantification of organic pollutant degradation in contaminated aquifers using compound specific stable isotope analysis - Review of recent developments. *Org. Geochem.* **2012**, *42* (12), 1440–1460.

(69) *Environmental Isotopes in Biodegradation and Bioremediation*; Aelion, C. M., Hohener, P., Hunkeler, D., Aravena, R., Eds.; CRC Press: Boca Raton, FL, 2010.